LA-UR- 10-02017

Approved for public release; distribution is unlimited.

Title:	Ionic liquid pretreatment of poplar wood at room temperature: Swelling and incorporation of nanoparticles
Author(s):	Marcel Lucas, Brian A. Macdonald, Gregory L. Wagner, Steven A. Joyce, and Kirk D. Rector
Intended for:	American Chemical Society Fall 2010 Meeting

Los Alamos
NATIONAL LABORATORY
EST. 1943

Form 836 (7/06)

Ionic liquid pretreatment of poplar wood at room temperature: Swelling and incorporation of nanoparticles

Marcel Lucas, Brian A. Macdonald, Gregory L. Wagner, Steven A. Joyce, and Kirk D. Rector

Chemistry Division, Los Alamos National Laboratory, Los Alamos, New Mexico 87545

Introduction

Lignocellulosic biomass represents a potentially sustainable source of liquid fuels and commodity chemicals. It could satisfy the energy needs for transportation and electricity generation, while contributing substantially to carbon sequestration and limiting the accumulation of greenhouse gases in the atmosphere. Potential feedstocks are abundant and include crops, agricultural wastes, forest products, grasses, and algae.[1,2] Among those feedstocks, wood is mainly constituted of three components: cellulose, hemicellulose, and lignin.[3] The conversion process of lignocellulosic biomass typically consists of three steps: 1) pretreatment; 2) hydrolysis of cellulose and hemicellulose into fermentable sugars; and 3) fermentation of the sugars into liquid fuels (ethanol) and other commodity chemicals. The pretreatment step is necessary due to the complex structure of the plant cell wall and the chemical resistance of lignin. Most current pretreatments are energy-intensive and/or polluting.[1,2] So it is imperative to develop new pretreatments that are economically viable and environmentally friendly.

Recently, ionic liquids have attracted considerable interest, due to their ability to dissolve biopolymers, such as cellulose,[4-8] lignin,[8-10] native switchgrass,[11] and.[3,8,12-14] Ionic liquids are also considered green solvents, since they have been successfully recycled at high yields for further use with limited efficiency loss. Also, a few microbial cellulases remain active at high ionic liquid concentration.[15] However, all studies on the dissolution of wood in ionic liquids have been conducted so far at high temperatures, typically above 90°C. Development of alternative pretreatments at room temperature is desirable to eliminate the additional energy cost.

In this study, thin sections of poplar wood were swollen at room temperature by a 3 h ionic liquid (1-ethyl-3-methylimidazolium acetate or EMIMAc) pretreatment. The pretreated sample was then exposed to an aqueous suspension of nanoparticles that resulted in the sample contraction and the deposition of nanoparticles onto the surface and embedded into the cell wall. To date, both silver and gold particles ranging in size from 40-100 nm have been incorporated into wood. Penetration of gold nanoparticles of 100 nm diameter in the cell walls was best confirmed by near-infrared confocal Raman microscopy,[16-18] since the deposition of gold nanoparticles induces a significant enhancement of the Raman signal from the wood in their close proximity, an enhancement attributed to the surface-enhanced Raman effect (SERS).[19] After rinsing with water, scanning electron microscopy (SEM) and Raman images of the same areas show that most nanoparticles remained on the pretreated sample. Raman images at different depths reveal that a significant number of nanoparticles were incorporated into the wood sample, at depths up to 4 μm, or 40 times the diameter of the nanoparticles. Control experiments on an untreated wood sample resulted in the deposition of nanoparticles only at the surface and most nanoparticles were removed upon rinsing. This particle incorporation process enables the development of new pretreatments, since the nanoparticles have a high surface-to-volume ratio and could be chemically functionalized. Other potential applications for the incorporated nanoparticles include isotope tracing, catalysis,[20] imaging agents,[21] drug-delivery systems,[22] energy-storage devices[20,23] and chemical sensors.[20,24]

Experimental

Materials. Transverse sections of poplar wood were prepared using a sliding microtome. The sections were dried in an oven for 4 h between two glass slides at 60°C to prevent curling. The ionic liquid, 1-ethyl-3-methylimidazolium acetate (EMIMAc), was purchased from Sigma-Aldrich (St. Louis, Missouri). Suspensions of 20 nm silver, 60 nm silver, 40 nm gold and 100 nm gold nanoparticles were purchased from BBInternational, Cardiff, United Kingdom.

Sample preparation. Two wood samples, ~5x5 mm2, were cut from the same microtome section of 30 μm thickness. One sample was immersed in EMIMAc for 3 h at room temperature. After the EMIMAc pretreatment, the wood sample was blotted with a Kimwipe. The samples were placed on glass cover slips and 5 mL of gold nanoparticles suspension was then deposited on the untreated sample and the pretreated sample. The samples were left to dry overnight in air. After the Raman images, the samples were rinsed with de-ionized water, left to dry overnight in air before further examination. Additionally, rectangular poplar samples were cut from 40 μm thick microtome sections.

Raman microscopy. The excitation for the Raman images was the 776 nm laser line of a Ti:Sapphire laser (Coherent Mira 900-P). The collimated beam was focused to a line and redirected to the back of an inverted microscope (Carl Zeiss Axiovert 200) by a Raman edge dichroic (z785rdc, Chroma Technology). A C-apochromat 63x (N.A. 1.2) water immersion objective (Carl Zeiss) focused the laser line to a line approximately 1 μm wide and 100 μm long on the sample, with a total power of 80 mW at the sample. The Raman signal was collected in a backscattering configuration, focused onto a Holospec f/2.2 spectrograph (Kaiser Optical Systems) and filtered with a Holographic SuperNotch-Plus Filter (Kaiser Optical Systems). The signal was then dispersed with a holographic grating (HSG-785-LF, Kaiser) and imaged with a liquid nitrogen-cooled CCD camera (Princeton Instruments, Trenton, NJ). The Raman images were acquired by moving the sample across the laser line by 0.5 μm steps. The exposure time for each line was two minutes. For the collection of Raman images at different depths, an additional pinhole was added to reduce out-of-focus signals from the sample. The objective was moved along the depth direction by 2 μm steps. The exposure time was 30 seconds for each line.

Data analysis. Each CCD image corresponds to the signal from a line on the sample, and consists of 256 spectra. Each spectrum was integrated from 1050 cm^{-1} to 1140 cm^{-1} to form one line of the resulting Raman image. For the Raman intensity depth profile of hot spots, the intensity of all pixels in a 2x2 μm^2 area around each spot was integrated for each image at a particular depth. To normalize the intensity depth profile, its minimum value was subtracted from it and it was then divided by its maximum value. The error bars represent the uncertainty on the position of the selected area.

Scanning Electron Microscopy. Scanning electron micrographs were acquired using a FEI Quanta 200FEG operating at an accelerating voltage of 30 kV with a backscatter detector.

X-Ray Fluorescence micro-spectroscopy. An Edax Eagle III energy dispersive X-ray fluorescence (XRF) microscope was used to quantify nanoparticle uptake by averaging fluorescence over areas of diameter 40-160 μm. The instrument uses an Rh source using settings of 40 kV accelerating voltage, 800 μA current, and 50 μs dwell time to sample the poplar samples. It was determined that K, Mn, and S are the most closely related to both the density and mass

of the poplar sample and appear to be homogeneous with material thickness or density. Sulfur concentration (2.30 keV) was selected as an indicator of poplar density. The determination of S and Ag (22.1 keV) concentrations was performed using a corrective baseline average algorithm.

Results and Discussion

After a 3 h EMIMAc pretreatment, cross-sectional area measurements of poplar wood cells found that after the 3h EMIMAc pretreatment, the cell wall areas increased by 60% to 100% and the lumen areas were reduced by 40% to 83%, depending on the original cell size in the dry wood. After the pretreatment, a gentle rinsing with de-ionized water led to the almost immediate re-opening of the lumen. The cell walls also contracted after rinsing with water, but at a slower pace. In contrast, the deposition of de-ionized water droplets on untreated poplar wood resulted only in a limited expansion of the wood, and the wood cells recovered their original sizes within 30 min after the water evaporated.

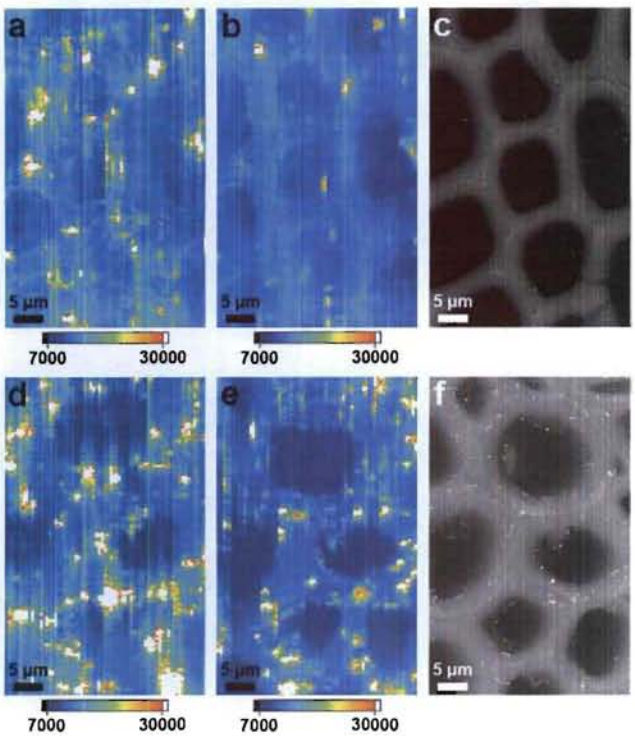

Figure 1. Raman and SEM images after deposition of gold nanoparticles on (a-c) an untreated sample and (d-f) a sample pretreated with 1-ethyl-3-methylimidazolium acetate for 3h. Following the deposition of nanoparticles, a Raman image was collected for each position (a,d). The samples were then rinsed with de-ionized water and Raman (b,e) and SEM (c,f) images were collected at the same positions.

The expansion of wood cells by an EMIMAc pretreatment and their subsequent contraction with water rinsing are the basis of a process to incorporate nanoparticles, and potentially other materials/chemicals, into the wood structure. To this effect, the water rinsing was replaced by the exposure of the EMIMAc-pretreated sample to an aqueous suspension of nanoparticles. XRF microspectroscopy was employed to quantify uptake and to test experimental conditions to maximize uptake. Experiments were conducted by varying the exposure time to EMIMAc (up to 4 hrs) followed by separate, fixed exposure to a suspension of Ag nanoparticles (1 or 4 hr). As a negative control, the poplar sample was exposed to the Ag suspension for one or four hours without EMIMAc pretreatment and rinsed to test for the possibility of Ag mechanical or electrostatic association. The XRF measurements indicated Ag presence in the control samples at the instrument detection limit, with slightly more Ag present when exposed for longer time, as might be expected. This is in agreement with the data shown in Figure 2 without EMIMAc pretreatment. In all experiments measured, exposure to both EMIMAc and Ag suspension resulted in at least an order of magnitude increase in the particle incorporation, again in rough agreement with the microscopy data shown in Figure 1. The data suggest that exposure to EMIMAc or Ag suspension longer than 1 hr only has a subsequently minor, increasing influence on particle incorporation. Further, increased exposure to Ag has a negligible or minor influence to particle incorporation at these timescales.

For the microscopy experiments, thin sections of poplar were pretreated for 3 hr with EMIMAc, and then exposed to a suspension of 100 nm gold nanoparticles. As a control experiment, an untreated poplar wood section was also exposed to the same suspension of nanoparticles. After the deposition of 100 nm gold nanoparticles, three Raman images were collected at different areas from the untreated sample and the one pretreated with EMIMAc (Figs. 1(a) and 1(d)). In addition to the cellulose Raman signal which reveals the wood cell walls, there are multiple hot spots (shown as white spots) attributed to the presence of gold nanoparticles or aggregates of nanoparticles. The Raman signal at these hot spots is significantly enhanced due to the field enhancement in close proximity of gold nanoparticles.[19] Using the same excitation, no noticeable enhancement was observed from 20 nm diameter silver nanoparticles deposited on wood, while only a small enhancement was observed for 60 nm silver and 40 nm gold nanoparticles. Therefore, only the 100 nm gold nanoparticles will be dealt with in the following discussion. All presented Raman images were obtained by integrating Raman spectra from 1050 cm^{-1} to 1140 cm^{-1}, a band that includes the cellulose peaks typically located around 1095 cm^{-1} and 1120 cm^{-1} in spontaneous Raman spectra (not enhanced by gold nanoparticles).[19] The density of hot spots on the untreated sample is comparable to the one on the pretreated sample. The same conclusion was reached for two other imaged areas (data not shown).

After the first series of Raman images, both samples were rinsed with de-ionized water at similar flow rates and left to dry overnight in air. A second series of Raman images at the same areas were collected after rinsing for direct comparison (Figs. 1(b) and (d)). Most hot spots on the untreated sample disappeared after rinsing. The rinsed sample pretreated with EMIMAc retained most hot spots. To confirm the removal of nanoparticles after rinsing, SEM images were collected from the same areas from both samples (Figs. 1(c) and (f)). The SEM images show that most nanoparticles were removed after rinsing from the untreated sample, while a high density of gold nanoparticles remained on the pretreated sample. On the rinsed untreated sample, the nanoparticles are mostly isolated. A few aggregates are observed and their size is typically below five nanoparticles. On the rinsed pretreated sample, the nanoparticles are rarely isolated and tend to form larger aggregates with 10 to 30 nanoparticles. Most nanoparticles and aggregates of nanoparticles observed on the SEM images of the pretreated sample yield a hot spot with variable enhancement on their corresponding Raman images. For the untreated sample, a large number of isolated nanoparticles and small aggregates yield no hot spot on the Raman

image. Overall, the Raman and SEM images showed no preferential deposition of nanoparticles in the cell corners, middle lamella or secondary cell walls.

After the second series of Raman images, but before the acquisition of SEM images, a series of Raman images at different depths from -4 to +6 μm were acquired from the areas shown in Fig. 1 for the untreated and pretreated samples. The intensity of all hot spots varies as the depth is changed. To determine whether the gold nanoparticles are adsorbed at the sample surface or incorporated deep inside the sample, the intensity of six and twelve hot spots was measured as a function of depth for the untreated sample and pretreated sample, respectively. Included in this study are all hot spots that could be tracked across the images at different depths.

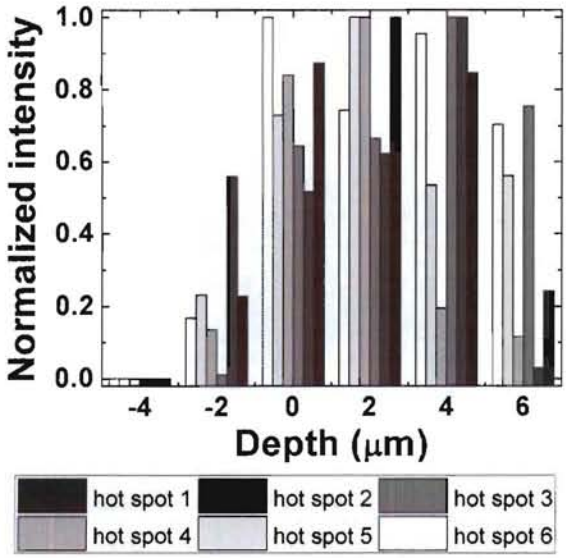

Figure 2. Raman intensity depth profile of six hot spots for the pretreated wood sample. The intensity profiles exhibit a maximum at positive depths, meaning that the corresponding nanoparticles are incorporated inside the sample.

For the untreated sample, the intensity of all hot spots reaches a maximum at a depth around 0 μm or at a negative depth. The depth 0 μm corresponds to the surface of the sample. Positive depths mean that the laser line is focused inside the sample. In the untreated sample, the nanoparticles producing hot spots are all at the surface. As for the pretreated sample, the intensity depth profiles of six hot spots from nanoparticles incorporated inside the sample are shown in Fig. 2. The hot spots 2 and 3 reach their maximum intensity at a depth of 4 μm. This depth is 40 times the diameter of the nanoparticle. From the data shown in Figs. 1 and 2, it is estimated that, for this area, at least 25% of nanoparticles on the pretreated sample are below the surface.

The incorporation of nanoparticles in the pretreated sample is attributed to the expansion of wood cells upon exposure to EMIMAc. Ionic liquids are known for their ability to disrupt the hydrogen-bonding network in wood, allowing them to diffuse inside cells.[3,12] The overall expansion and disruption of hydrogen bonding increased the distance between polymer chains inside the wood structure, paving the way for the incorporation of nanoparticles. The contraction of the cell walls after rinsing ensured that the nanoparticles would remain on the sample even after rinsing. As for the untreated sample, water tends to adsorb on cellulose and hemicellulose by forming hydrogen bonds.[28] The more limited expansion of untreated wood samples and the formation of hydrogen bonds restrict the access of nanoparticles inside the sample. The nanoparticles at the surface of the untreated sample are only weakly adsorbed and can be easily washed away upon rinsing.

Conclusions

A microtome section of poplar wood was swollen by a 3h ionic liquid (1-ethyl-3-methylimidazolium acetate) pretreatment. The pretreated sample was then exposed to an aqueous suspension of gold nanoparticles of 100 nm diameter, that resulted in the sample contraction and the deposition of nanoparticles as confirmed by Raman images. After rinsing with water, SEM and Raman images of the same areas show that most nanoparticles remained on the sample. Raman images at different depths reveal that at least 25% of deposited nanoparticles were incorporated into the wood sample, at depths up to 4 μm. Control experiments on untreated wood samples resulted in the deposition of nanoparticles only at the surface and most nanoparticles were removed upon rinsing. Quantitative X-ray fluorescence microanalyses indicate that the majority of nanoparticle incorporation occurs after an ionic liquid pretreatment shorter than 1 hr. This particle incorporation process based on the swelling/contraction of the wood and the disruption of its hydrogen-bond network enables isotope tracing, the development of new sensing, imaging capabilities and pretreatments.

Acknowledgement. This study was funded by a Laboratory Directed Research and Development grant from Los Alamos National Laboratory (20080001DR). The authors acknowledge Dr. Paul Langan (Los Alamos National Laboratory) and Prof. Constance Schall (Univ. Toledo) for useful discussions.

References

(1) Banerjee, S.; Mudliar, S.; Sen, R.; Giri, B.; Satpute, D.; Chakrabarti, T.; Pandey, R. A. *Biofuels, Bioprod. Biorefin.* **2010**, *4*, 77.
(2) Huber, G. W.; Iborra, S.; Corma, A. *Chem. Rev.* **2006**, *106*, 4044.
(3) Kilpeläinen, I.; Xie, H.; King, A.; Granstrom, M.; Heikkinen, S.; Argyropoulos, D. S. *J. Agric. Food Chem.* **2007**, *55*, 9142.
(4) Pinkert, A.; Marsh, K. N.; Pang, S.; Staiger, M. P. *Chem. Rev.* **2009**, *109*, 6712.
(5) Dadi, A. P.; Varanasi, S.; Schall, C. A. *Biotechnol. Bioeng.* **2006**, *95*, 904.
(6) Dadi, A. P.; Schall, C. A.; Varanasi, S. *Appl. Biochem. Biotechnol.* **2007**, *136-140*, 407.
(7) Kosan, B.; Michels, C.; Meister, F. *Cellulose* **2008**, *15*, 59.
(8) Lee, S. H.; Doherty, T. V.; Linhardt, R. J.; Dordick, J. S. *Biotechnol. Bioeng.* **2009**, *102*, 1368.
(9) Tan, S. S. Y.; MacFarlane, D. R.; Upfal, J.; Edye, L. A.; Doherty, W. O. S.; Patti, A. F.; Pringle, J. M.; Scotta, J. L. *Green Chem.* **2009**, *11*, 339.
(10) Pu, Y.; Jiang, N.; Ragauskas, A. J. *J. Wood Chem. Technol.* **2007**, *27*, 23.
(11) Singh, S.; Simmons, B. A.; Vogel, K. P. *Biotechnol. Bioeng.* **2009**, *104*, 68.
(12) Xie, H.; King, A.; Kilpelainen, I.; Granstrom, M.; Argyropoulos, D. S. *Biomacromolecules* **2007**, *8*, 3740.
(13) Fort, D. A.; Remsing, R. C.; Swatloski, R. P.; Moyna, P.; Moyna, G.; Rogers, R. D. *Green Chem.* **2007**, *9*, 63.
(14) Sun, N.; Rahman, M.; Qin, Y.; Maxim, M. L.; Rodríguez, H.; Rogers, R. D. *Green Chem.* **2009**, *11*, 646.
(15) Pottkämper, J.; Barthen, P.; Ilmberger, N.; Schwaneberg, U.; Schenk, A.; Schulte, M.; Ignatiev, N.; Streit, W. R. *Green Chem.* **2009**, *11*, 957.
(16) Agarwal, U. P. *Planta* **2006**, *224*, 1141.
(17) Gierlinger, N.; Schwanninger, M. *Spectroscopy* **2007**, *21*, 69.
(18) Schenzel, K.; Almlöf, H.; Germgård, U. *Cellulose* **2009**, *16*, 407.
(19) Agarwal, U. P.; Reiner, R. S. *J. Raman Spectrosc.* **2009**, *40*, 1527.
(20) Trindade, T.; O'Brien, P.; Pickett, N. L. *Chem. Mater.* **2001**, *13*, 3843.
(21) Jain, P. K.; Lee, K. S.; El-Sayed, I. H.; El-Sayed, M. A. *J. Phys. Chem. B* **2006**, *110*, 7238.
(22) Gupta, A. K.; Gupta, M. *Biomaterials* **2005**, *26*, 3995.
(23) Sun, B.; Marx, E.; Greenham, N. C. *Nano Lett.* **2003**, *3*, 961.

(24) Nowak-Lovato, K. L.; Rector, K. D. *Appl. Spectrosc.* **2009**, *63*, 387.
(25) Misra, M. K.; Ragland, K. W.; Baker, A. J. *Biomass Bioenergy* **1993**, *4*, 103.
(26) Khan, I.; Cunningham, D.; Graham, D.; McComb, D. W.; Smith, W. E. *J. Phys. Chem. B* **2005**, *109*, 3454.
(27) Basu, S.; Pande, S.; Jana, S.; Bolisetty, S.; Pal, T. *Langmuir* **2008**, *24*, 5562.
(28) Olsson, A.-M.; Salmén, L. *Carbohydr. Res.* **2004**, *339*, 813.